

# Synthesis of Novel Ferrite Foam Material for Water-Splitting Application

Rajesh Shende, Jan Puszynski,\* Michael Opoku, Rahul Bhosale

Department of Chemical and Biological Engineering,  
South Dakota School of Mines & Technology,  
Rapid City, SD 57701 USA, Jan.Puszynski@sdsmt.edu

## ABSTRACT

This paper reports the synthesis of ferrite material with foam-like morphology that anticipated to have extraordinary potential towards  $H_2$  generation from high temperature water-splitting reaction. The material was synthesized using a modified sol-gel method involving the addition of polymer microspheres into the gel followed by fast microwave heating. Powder X-ray diffraction (XRD), scanning electron microscopy (SEM), and BET surface area analysis were performed to characterize the ferrite material. Energy dispersive spectroscopy indicated that the material was free of any carbon impurities whereas SEM images distinctly exhibited the foam-like morphology. Ferrite was also synthesized by powder processing approach where the constituent powders were mixed in an attritor mill and sintered in  $N_2$  atmosphere. As-synthesized ferrites were effective in generating  $H_2$  from water-splitting reaction at  $1000^\circ\text{C}$ .

**Keywords:** Ferrite foam, sol-gel, nanotubular structure, high surface area, water-splitting

## 1 INTRODUCTION

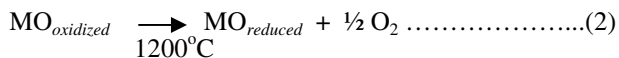
Thermolysis of water (water-splitting in absence of chemical compounds) is extremely challenging as the direct thermal dissociation of water requires very high temperatures ( $>2500^\circ\text{C}$ ) in order to accomplish a significant conversion [1]. This process has a rather minimal chance for commercialization, due to extreme conditions of the process and the need for developing unique high temperature membrane technology for separation of hydrogen and oxygen. In contrast, a thermochemical process that utilize metal oxide (MO)-based redox reactions may be conducted at significantly lower temperatures without the use of membrane separation. Therefore, this process seems to be by far more technically feasible for generation of hydrogen by water molecule splitting.

The thermochemical water-splitting is a two-step process, which utilizes redox reactions of mixed valence metal oxides (MO) [2-5]. In the first step the reduced MO ( $MO_{reduced}$ ) is oxidized at elevated temperatures by taking

oxygen from water and producing hydrogen, water splitting reaction (1):



In the second step the oxidized MO ( $MO_{oxidized}$ ) is converted back into its original reduced form so that it can be reused again (regeneration or oxygen desorption), releasing oxygen during regeneration according to the following reaction (2):



Reaction (1) is slightly exothermic whereas Reaction (2) is endothermic. The advantage of a two-step process is that the production of pure hydrogen and removal of oxygen are conducted in separate steps, avoiding the need for high-temperature separation of oxygen and hydrogen (as desired in thermolysis) and the possibility of explosive mixture formation. The disadvantage of the process is that it requires cycling of the water-splitting and regeneration steps. Further disadvantage is that the water-splitting requires typically lower temperatures as compared with the regeneration step, which takes place at relatively higher temperatures by few hundreds of Celsius degree.

So far, the materials that have been investigated for the water-splitting application are mainly the redox pair such as  $Fe_3O_4/FeO$  [6],  $Mn_3O_4/MnO$  [7],  $ZnO/Zn$  [8],  $TiO_2/TiO_x$  ( $x < 2$ ) [9] and doped ferrites [10,11]. Among these materials, ferrites such as  $(A_xB_y)Fe_2O_4$  (doped spinel) or  $A_xB_yFe_{1-x-y}O$  (doped wustite) or their mixtures with elements A and B being bivalent metal cations such as Mn, Ni or Zn [2] were reported to be most active materials for hydrogen generation from water-splitting. Using Ni and Mn doped-ferrites, the temperature needed for a water splitting was decreased to  $627^\circ\text{C}$ , however, the regeneration temperature was still too high ( $>1300^\circ\text{C}$ ) [12]. Thus, even if doping to some extent is effective, the temperature difference between both steps of the cycle is significant.

Synthesis of various ferrites have been reported by solid-state synthesis, self-propagation high temperature (SHS) synthesis method, and aerosol spray pyrolysis [2,13]. Several ferrites synthesized by these methods are in the

powder form, which is mostly non-porous yielding low surface area. During regeneration step at higher temperatures the surface area further decreases due to grain growth, which will provide less number of active sites for oxygen scavenging. When the ferrite material is synthesized in a porous form (e.g. foam), high surface area can be achieved.

In this study, we report synthesis of ferrite foam-like material using sol-gel synthesis approach involving the use of polymer microspheres with hydrocarbons present inside the core that are surrounded by a polymer shell.

## 2 EXPERIMENTAL

### 2.1 Synthesis of ferrites

In one approach,  $\text{TiO}_2$ ,  $\text{ZnO}$ , and  $\text{Fe}_2\text{O}_3$  powders were combined at predetermined concentration levels and later mixed in an attritor mill for 1 h in water. The powder after milling were dried and sintered at  $1000^\circ\text{C}$  for 1 hr in  $\text{N}_2$  environment.

In another approach, sol-gel method was employed to synthesize the redox materials. In the synthesis, Sn, Ni, and Fe salts were dissolved in ethanol by means of sonication. Into this solution, propylene oxide was added and the solution was left undisturbed to form a gel. The gel formation was noticed after 5 min. To prepare the foam, the gel was mixed with 10 wt% polymer microspheres (from Akzo Nobel). The interior of polymer spheres contains hydrocarbon gases surrounded by a shell, which is only a micron thick. It is made up of a thermoplastic polymer. The ferrite gel containing these microspheres was fired rapidly in an industrial scale microwave furnace (VIS 300-01B, 5kW CPI Company) in air atmosphere at  $1000$ - $1200^\circ\text{C}$  for 5-10 minutes and cooled down.

### 2.2 Characterization of ferrites

Powder X-ray diffraction, scanning electron microscopy (SEM), energy dispersive spectral analysis, and BET surface area measurement were performed to characterize the synthesized ferrite materials.

### 2.3 Water-splitting reaction

Thermochemical water-splitting reaction was performed in a quartz tubular isothermal reactor (0.9 inch I.D.) supported in a high-temperature split furnace. The quartz tube was connected to two mass flow controllers (AALBORG, Inc with flow range of 0-1000  $\text{smL/min}$ ) to monitor the flow rate of inert gases. About 5.0 g of redox material was loaded inside an alumina boat type sample holder and pushed inside a quartz reactor. At the inlet, a water reservoir was connected using  $\frac{1}{4}$ " sized tubing. At the outlet of a reactor, a water absorbent packed column was installed. Redox material was heated to  $1000^\circ\text{C}$  under

constant flow of  $\text{N}_2$ . Water was heated and the steam was allowed to pass over the material present inside an alumina boat. The effluent gas stream from a reactor was sampled continuously using a gas syringe.

## 2.4 Gas-chromatography

The gaseous effluents from a reactor were analyzed on HP6890 Gas chromatograph provided with Chrompack column and thermal conductivity detector (TCD).  $\text{H}_2$  concentration was determined from the calibration curve.

## 3 RESULTS AND DISCUSSION

Prior to ferrite foam synthesis, a powder processing approach was adopted to synthesize redox material with wustite and spinel crystalline phases. To prepare this material,  $\text{TiO}_2$ ,  $\text{ZnO}$ , and  $\text{Fe}_2\text{O}_3$  powders were combined and mixed in an attritor mill. The powder after milling in an attritor were dried and sintered at  $1000^\circ\text{C}$  for 1 hr in  $\text{N}_2$  environment. SEM images of the sintered powder is shown in Figure 1 showing smaller and relatively bigger irregular sized grains. Some grains appear to be faceted as well.

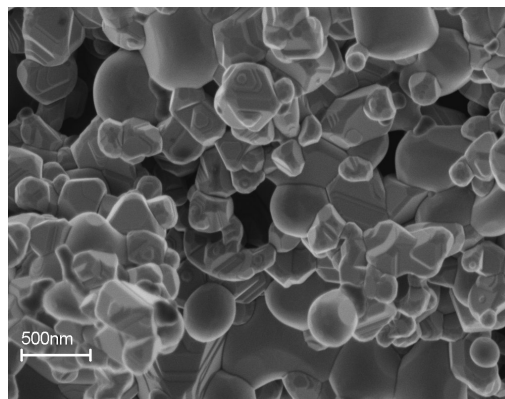


Figure 1: SEM images of a redox material prepared by attrition milling.

Doping ferrites with several metals should increase the possibility of having more oxygen vacancies as compared with the one without dopant. In other words, improved enhancement in water-splitting capability is expected if higher concentration of oxygen vacancies is present in the crystal lattices (lattice defects). When multivalent metal such as Ti is added to ferrite, the possibilities of adding defects will be enhanced because of the formation of distorted spinel nanocrystals. If the mixture of spinel and wustite of Ti-based ferrites is prepared, more distorted structure and high oxygen vacancies should be achieved, which should help in narrowing the temperature difference between water splitting and regeneration steps.

The X-ray diffraction pattern of the binary redox material prepared using attrition milling approach is depicted in Figure 2. The peak positions resemble to the  $\text{ZnFe}_2\text{O}_4$  and  $\text{Fe}_2\text{ZnTi}_3\text{O}_{10}$  phases. Basic calculations for

$\text{ZnFe}_2\text{O}_4$  phase reveal reflections corresponding to 220, 311, 222, 400, 422, 511, 620, 533, 622, 444, 642, and 533 lattice planes. These reflections match with those of the wustite crystal structure. Quantitative estimation indicates that the  $\text{ZnFe}_2\text{O}_4$  phase is about 85%, whereas  $\text{Fe}_2\text{ZnTi}_3\text{O}_{10}$  is a remaining phase. The X-ray peak positions corresponding to these phases are identical to those documented by the International Center for Diffraction Data (ICDD) and are also inserted into the same figure.

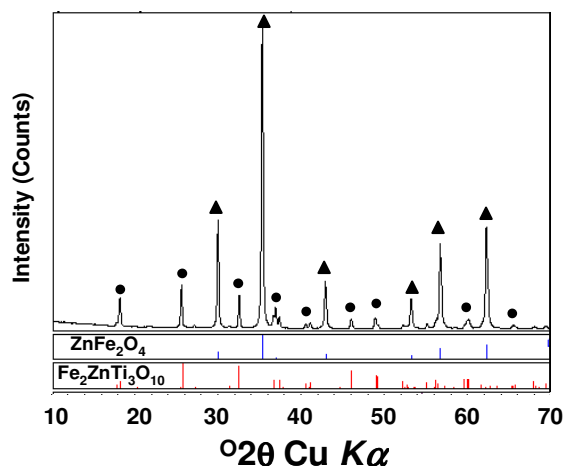


Figure 2: powdered x-ray diffraction pattern of the redox material showing  $\text{ZnFe}_2\text{O}_4$  (▲) and  $\text{Fe}_2\text{ZnTi}_3\text{O}_{10}$  (●) phases.

Presence of two different crystalline phases was validated by the x-ray mapping during SEM analysis. The phase contrasting image is presented in Figure 3, which shows distribution of  $\text{ZnFe}_2\text{O}_4$  and  $\text{Fe}_2\text{ZnTi}_3\text{O}_{10}$  phases. Such material will be highly desirable for water-splitting reaction as they tend to scavenge oxygen more easily and therefore generate hydrogen. However, as this ferrite material exists in the powder form with sufficiently large particle sizes (see Figure 1), the available surface for the irreversible binding of oxygen is very limited.

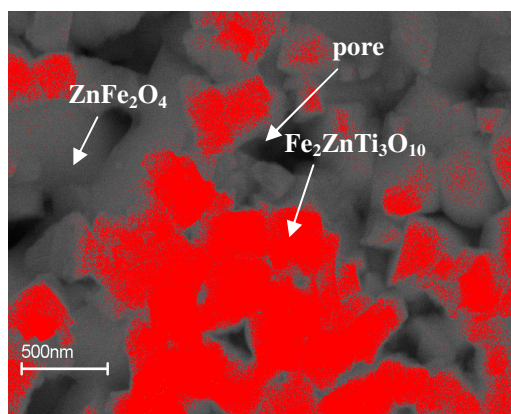


Figure 3: SEM image (back scattered) with phase contrast showing  $\text{ZnFe}_2\text{O}_4$  and  $\text{Fe}_2\text{ZnTi}_3\text{O}_{10}$  phases.

If ferrite is synthesized as a porous material, high surface area can be achieved. Synthesis method for ferrite with foam-like morphology was developed using the sol-gel methodology where Sn, Ni and Fe salts were dissolved in ethanol by sonication and to this solution, propylene oxide was added. After the gel formation, about 10 wt% polymer microspheres were added. A well-mixed ferrite gel containing these microspheres was fired rapidly in an industrial scale microwave furnace at about 1000-1200°C and quenched in air. The SEM image of the product is presented in Figure 4, which clearly exhibits foam-like morphology.

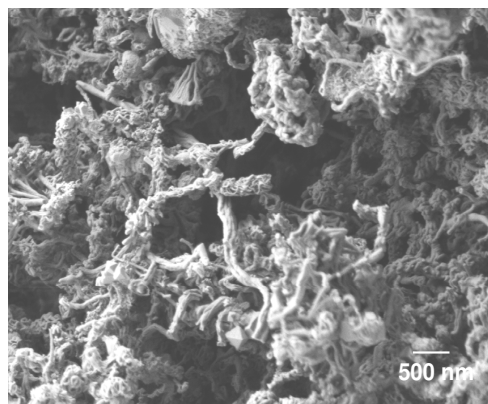


Figure 4: SEM image of  $\text{Sn}_{0.5}\text{Ni}_{0.5}\text{Fe}_2\text{O}_4$  ferrite.

The energy dispersive spectrum of the above material indicates the presence of Sn, Fe, and Ni throughout the sample matrix. One can argue that the structure resembles to fibrous foam-like morphology. After rigorous analysis, it was found out that the few fibers in the foam have nanoscale tubular structure. The SEM image presented in Figure 5 shows that the tubes in the foam are several  $\mu\text{m}$  long and an insert presented in the upper right hand corner hints that some of the tubes might be hollow.

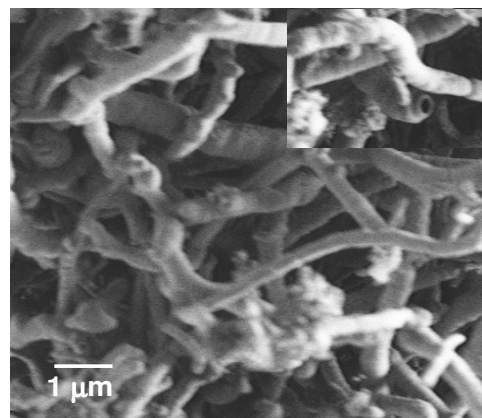


Figure 5: SEM image of the ferrite showing that the tubes in the foam are several  $\mu\text{m}$  in length.

The BET surface area of this foam was greater than 100 m<sup>2</sup>/g, which is several times higher than the Ni-Zn ferrites reported by others (36 m<sup>2</sup>/g) [14]. It will be interesting to analyze the phase composition of these fiber-like foams by x-ray analysis. We expect presence of two distorted crystalline phases in this material, which will need further investigation.

Thermochemical water-splitting was performed in a quartz tubular isothermal reactor supported in a high-temperature split furnace as described in the Experimental Section. The effluent gas stream from a reactor was sampled continuously by a gas syringe and analyzed using gas-chromatography provided with a thermal conductivity detector (TCD). The analysis indicated evolution of H<sub>2</sub>, which was increased continuously during the course of experiment for about 45 min.

Studies are in progress to understand how ferrite foam-like structures are formed during fast microwave heating and quenching. Furthermore, we are trying to understand their effectiveness towards water-splitting.

## 4 CONCLUSIONS

Synthesis of ferrite containing wustite and spinel phases has been successfully demonstrated by mixing the powder materials in an attritor mill followed by sintering at 1000°C in N<sub>2</sub> environment. Modified sol-gel method involving the addition of polymer microspheres in the ferrite gel produced fibrous foam-like material with nanoscale tubular structure after rapid heating in a microwave furnace. When these ferrite materials were used for water-splitting reaction, evolution of H<sub>2</sub> was confirmed using the gas-chromatography. The BET surface area of the foam-like material was in excess of 100 m<sup>2</sup>/g, which is several times higher than the ferrites conventionally used in water-splitting reaction and therefore, it is believed that the ferrite foam has tremendous potential for generating H<sub>2</sub> from water-splitting reaction.

## ACKNOWLEDGEMENT

The authors gratefully acknowledge the financial support by the National Science Foundation, Grant No. CBET-0756214.

## REFERENCES

- [1] A.T-Raissi, N. Muradov, C. Huang, and O. Adebiyi, Transactions of ASME, 129, 184, 2007.
- [2] C.C. Agrafiotis, C. Pagkoura, S. Lorentzou, M. Kostoglou, A.G. Konstandopoulos, Catalysis Today, 127, 265, 2007.
- [3] A. Steinfeld, Solar Energy, 78, 603, 2005.
- [4] Y. Tamaura, A. Steinfeld, P. Kuhn, K. Ehrensberger, Energy, 20, 325, 1995.
- [5] C. Perkins, A.W. Weimer, International Journal of Hydrogen Energy, 29, 1587, 2004.
- [6] A. Steinfeld, S. Sanders, R. Palumbo, Solar Energy, 65., 43, 1999.
- [7] M. Sturzenegger, P. Nuesch, Energy, 24, 959, 1999.
- [8] A. Steinfeld, International Journal of Hydrogen Energy, 27, 611, 2002.
- [9] A. Steinfeld, R. Palumbo, Encyclopedia of Physical Science & Technology, R.A. Mayers Ed., Academic Press, 15, 237, 2001.
- [10] Y. Tamaura, N. Hasegawa, M. Kojima, Y. Ueda, H. Amano, M. Tsuji, Energy, 23, 879, 1998.
- [11] M. Kojima, T. Sano, Y. Wada, T. Yamamoto, M. Tsuji, Y. Tamaura, Journal of Physical Chemistry of Solids, 57, 1757, 1996.
- [12] Y. Tamaura, M. Kojima, Y. Ueda, N. Hasegawa, M. Tsuji, International Journal of Hydrogen Energy, 23, 1185, 1998.
- [13] C. Agrafiotis, M. Roeb, A.G. Konstandopoulos, L. Nalbandian, V.T. Zaspalis, C. Sattler, P. Stobbe, A.M. Steele, Solar Energy, 79, 409, 2005.
- [14] Y.-P. Fu, C.-H. Lin, Journal of Magnetism and Magnetic Materials, 251, 74, 2002.